Indonesian Journal of Biotechnology

VOLUME 31(1), 2026, 49-61 | RESEARCH ARTICLE

The role of astaxanthin-Cu^{2+} in stabilizing glycated human serum albumin for type 2 diabetes mellitus management: a computational approach

Naufal Abiyyu[1], Alfia Fitrianita[2], I Made Artika[1], Josephine Elizabeth Siregar[3], Syahputra Wibowo[3,*], Bantari Wisynu Kusuma Wardhani[4], Canggih Setya Budi[5], Tri Rini Nuringtyas[6,*]

[1]Department of Biochemistry, Faculty of Mathematics and Natural Sciences, Bogor Agricultural University, Dramaga Campus, Bogor 16680, Indonesia
[2]Biotechnology study program, Postgraduate school, Bogor Agricultural University, Dramaga Campus, Bogor 16680, Indonesia
[3]Eijkman Research Center for Molecular Biology, National Research and Innovation Agency (BRIN), Cibinong, Bogor 16911, Indonesia
[4]Research Center for Pharmaceutical Ingredients and Traditional Medicine, National Research and Innovation Agency (BRIN), Bogor, Indonesia
[5]Research Center for Polymer Technology, National Research and Innovation Agency (BRIN), The B.J. Habibie Science and Technology Area, South Tangerang, Banten 15314, Indonesia
[6]Department of Tropical Biology, Faculty of Biology, Universitas Gadjah Mada, Yogyakarta, Indonesia
*Corresponding author: syah031@brin.go.id; tririni@ugm.ac.id

SUBMITTED 29 July 2025 **REVISED** 9 March 2026 **ACCEPTED** 12 March 2026

ABSTRACT Type 2 diabetes mellitus (T2DM) leads to the non-enzymatic glycation of proteins, resulting in the formation of advanced glycation end products (AGEs), which contribute to diabetic complications. Human serum albumin (HSA), a major plasma protein, undergoes structural alterations upon glycation (gHSA), reducing its stability and biological functions. Astaxanthin (ASX), a potent antioxidant, is limited by its instability and moderate binding affinity. In this study, we explore the use of copper (Cu^{2+}) to form a stable ASX-Cu^{2+} complex, enhancing the antioxidant properties of ASX and improving its interaction with HSA and gHSA. Utilizing computational approaches such as molecular docking, molecular dynamics (MD) simulations, and free energy landscape (FEL) mapping, we analyze the stability and conformational changes of HSA and gHSA upon binding with ASX and ASX-Cu^{2+}. The residue interaction network (RIN) analysis reveals that ASX-Cu^{2+} complexes create a more robust and interconnected network of non-covalent interactions, particularly enhancing hydrogen bonding, π-stacking, and ionic interactions. The ASX-Cu^{2+} complex at a 1:2 molar ratio significantly improved the binding affinity and structural stability of both native and glycated HSA, reducing protein fluctuations and promoting a more compact conformation. These findings suggest that ASX-Cu^{2+} complexes offer therapeutic potential for stabilizing albumin under glycation-induced stress, with implications for managing oxidative stress and diabetes-related complications.

KEYWORDS Astaxanthin, Cu^{2+}, Diabetes mellitus, T2DM, gHSA

1. Introduction

Type 2 diabetes mellitus (T2DM) is a globally prevalent metabolic disorder characterized by chronic hyperglycaemia that promotes non-enzymatic glycation of circulating proteins and the formation of advanced glycation end products (AGEs), which contribute to diabetic complications (Khalid et al. 2022). Human serum albumin (HSA), the most abundant plasma protein, serves as a major carrier of endogenous and exogenous ligands such as fatty acids, nucleic acids, hormones, metals, toxins, and drugs, and plays an important role in the antioxidant capacity of plasma (De Simone et al. 2021). However, glycation alters the structure of HSA, producing glycated HSA (gHSA) that exhibits reduced ligand binding, impaired antioxidant activity, and increased aggregation, thereby compromising its stability and biological functions and contributing to oxidative stress in diabetic conditions (Jeevanandam et al. 2024).

Astaxanthin (ASX), a xanthophyll carotenoid with strong reactive oxygen species (ROS) scavenging ability, has attracted attention as a natural antioxidant with therapeutic potential (Valko et al. 2007). Its antioxidant activity is attributed to a conjugated polyene chain and terminal hydroxyl (-OH) and keto (=O) groups that facilitate electron donation and free radical stabilization (Guérin et al. 2003; Ambati et al. 2014). However, the inherent instability and moderate binding affinity of free ASX may limit its bio efficacy. The presence of oxygen-containing functional groups also enables ASX to coordinate with tran-

sition metal ions such as Cu^{2+}, forming stable complexes that may enhance molecular stability and bioavailability, making them promising candidates for applications in drug delivery and bioinorganic systems (Shen et al. 2020).

Recent studies have explored metal complexation strategies with transition metals such as copper (Cu^{2+}) to enhance antioxidant activity and molecular stability (Wibowo et al. 2022) The ASX-Cu^{2+} complex is therefore hypothesized to improve interactions with target proteins and increase resistance to glycation-induced structural alterations. To investigate this, we employed an integrated computational approach combining molecular docking, molecular dynamics (MD) simulations, radius of gyration analysis, residue interaction network (RIN), and free energy landscape (FEL) mapping to evaluate the structural stability, binding affinity, and interaction patterns of HSA and gHSA with the ASX-Cu^{2+} complex. These methods provide atomistic insights into protein-ligand interactions that are difficult to obtain experimentally, enabling prediction of the stabilizing effects of ASX-Cu^{2+} and supporting the development of therapeutic strategies for mitigating glycation-related dysfunctions in diabetes.

2. Materials and Methods

2.1. Data mining

The study, performed from July to December 2024 at the National Research and Innovation Agency (BRIN) in Cibinong, Indonesia, used HSA protein structure data (PDB ID 4K2C). gHSA was made by complexing HSA with glucose (Pubchem ID 79025). Astaxanthin (PubChem ID 5281224) and Cu^{2+} (PubChem ID 27099), were obtained from Pubchem.

2.2. Molecular docking

Molecular docking simulations were performed using CB-Dock 2.0, a blind docking web server that automatically identifies potential ligand-binding sites and predicts binding poses without prior knowledge of the binding pocket. CB-Dock integrates the CurPocket cavity detection algorithm with the AutoDock Vina docking engine to enable efficient docking of small molecules to protein targets (Liu et al. 2022). CurPocket identifies potential binding cavities by analyzing local surface curvature and geometric features of the protein structure, allowing systematic exploration of ligand-accessible pockets independent of predefined grid boxes or known binding sites (Ke et al. 2025).

The three-dimensional structures of human serum albumin (HSA) and glycated HSA (gHSA) were obtained in PDB format, while astaxanthin (ASX) and the ASX-Cu^{2+} complexes were prepared in PDB format. In this study, Cu^{2+} was not modeled as a free solvated ion but as part of a coordinated bioinorganic complex with astaxanthin (ASX-Cu^{2+}). Consequently, the docking simulations treated the ASX-Cu^{2+} complex as a single ligand entity interacting with the protein binding pocket rather than modeling Cu^{2+} independently. CB-Dock automatically generated docking boxes for detected cavities, and docking simulations using AutoDock Vina produced multiple binding poses ranked by predicted binding free energy. The best poses, selected based on docking score and geometric consistency, were used as starting structures for molecular dynamics simulations. CB-Dock 2.0 has been reported to achieve approximately 85% accuracy in predicting correct binding poses with RMSD values below 2.0 Å (Liu et al. 2022).

2.3. Molecular dynamics

The docking results were further analyzed using the CABS-flex 2.0 web server (http://biocomp.chem.uw.edu.pl/CABSflex2) for molecular dynamics simulations. CABS-flex employs the CABS coarse-grained protein model, where each amino acid residue is represented by four pseudo-atoms and solvent effects are treated implicitly, reducing the degrees of freedom and generating a smoother energy landscape compared with classical all-atom simulations (Kuriata et al. 2018). This approach accelerates conformational sampling while still capturing large-scale protein motions and flexibility profiles (Jamroz et al. 2013). Visualization and analysis were performed using 3Dmol and D3 tools (Kuriata et al. 2018). In this study, Cu^{2+} was not treated as a free ion interacting independently with the protein but as part of a coordinated bioinorganic complex with astaxanthin (ASX-Cu^{2+}); therefore, the ASX-Cu^{2+} complex was modeled as a single ligand entity interacting with HSA and gHSA within the simulation system.

Molecular dynamics simulations were performed using 50 cycles and 50 trajectory frames over 10 ns, and the resulting trajectories were used to calculate root mean square fluctuation (RMSF). This simulation time was considered sufficient for evaluating protein flexibility, residue-level fluctuations, global compactness, and free energy landscape (FEL) characteristics rather than atomistic kinetic processes. The simulations produced stable RMSF profiles, consistent radius of gyration values, and well-defined energy basins, indicating adequate convergence of the conformational ensembles. Similar simulation durations are commonly used in CABS-flex studies and show good agreement with experimental observations and longer all-atom simulations for analyzing protein structural dynamics (Jamroz et al. 2013; Kuriata et al. 2018).

2.4. Gyration analysis

To evaluate protein compactness and conformational dynamics, the radius of gyration (Rg) was calculated from molecular dynamics (MD) trajectory snapshots. The estimation was performed using the HullRad algorithm, which constructs a convex hull around the molecular structure to approximate its hydrodynamic radius from atomic coordinates. This coarse-grained geometric approach provides reliable estimates for both folded and disordered biomolecules (Fleming and Fleming 2018). Ten representative frames from the MD simulations were analyzed by

uploading coordinate files to the HullRad web server (http://52.14.70.9/Run_hullrad.html). The resulting Rg values were used to assess structural compactness and conformational stability throughout the simulation.

2.5. Free energy landscape (FEL)

The conformational stability and heterogeneity of the system were analyzed using the free energy landscape (FEL) derived from molecular dynamics trajectories. FEL maps the energy minima and transition regions, allowing identification of the most probable conformational states. To construct the FEL, principal component analysis (PCA) was applied to the MD trajectories to reduce the high-dimensional data into the first two principal components (PC1 and PC2), which served as reaction coordinates (Sittel and Stock 2018). This approach enables the identification of metastable conformations and transition pathways, providing insight into the thermodynamic landscape and structural dynamics of the system.

2.6. Residue interaction network

Residue interaction network (RIN) analysis was performed to investigate the non-covalent interaction architecture of native and glycated human serum albumin (HSA and gHSA) in complex with astaxanthin-Cu^{2+} ligands. The protein-ligand structures obtained from molecular docking were uploaded in PDB format to the RINmaker web server (https://rinmaker.dais.unive.it/) to generate interaction networks. In this representation, each amino acid residue is treated as a node, while edges correspond to non-covalent interactions such as hydrogen bonds, van der Waals contacts, ionic interactions, hydrophobic contacts, π-π stacking, and cation-π interactions (Tiberti et al. 2022). The analysis was conducted using the default geometric and distance parameters provided by RINmaker. The resulting networks were visualized on the platform and exported in GraphML format for further comparative and topological analysis. This approach enabled the identification of key interaction patterns and residues involved in structural stabilization affected by glycation and ligand binding.

3. Results and Discussion

3.1. Molecular docking

The molecular docking analysis revealed distinct interaction patterns and binding affinities between astaxanthin (ASX), its copper complexes, and both native human serum albumin (HSA) and glycated HSA (gHSA) (Figure 1). The HSA-ASX complex showed a binding affinity of –10.2 kcal/mol, involving residues LEU115, LYS159, ALA126, and ALA176 through hydrogen bonding and hydrophobic interactions (Yin et al. 2023). Complexation with Cu^{2+} at a 1:2 ratio slightly increased the affinity to –10.4 kcal/mol, introducing additional interactions with ALA126, ILE142, and ARG144, including metal-acceptor and π-alkyl contacts (Wibowo et al. 2022). The strongest binding was observed for the HSA-ASX-Cu^{2+} (3:1) complex with a binding affinity of –12.3 kcal/mol, involving residues TYR138, ILE142, ARG114, and MET123, indicating enhanced stability due to multivalent metal coordination (Table 1). The molecular structures of the ASX-Cu^{2+} complexes used in the docking simulations are shown in Figure 1G (1:2 coordination ratio) and Figure 1H (3:1 coordination ratio).

For glycated HSA, glycation appeared to reduce the overall binding affinity. The gHSA-ASX complex showed a lower binding affinity of –9.5 kcal/mol, likely due to structural alterations in the protein that reduced ligand accessibility or affinity (Jeevanandam et al. 2024). Key interactions in this complex involved ALA126, ARG114, and PHE134. However, upon complexation with Cu^{2+} at a 1:2 ratio, the binding affinity improved to –10.0 kcal/mol. The ASX-Cu^{2+} (1:2) complex formed interactions with TYR138, LYS137, GLU565, and HIS146, suggesting that metal coordination may partially compensate for the loss of binding capacity due to glycation. The gHSA-ASX-Cu^{2+} (3:1) complex further improved in affinity to –11.6 kcal/mol and engaged with residues such as TYR140,

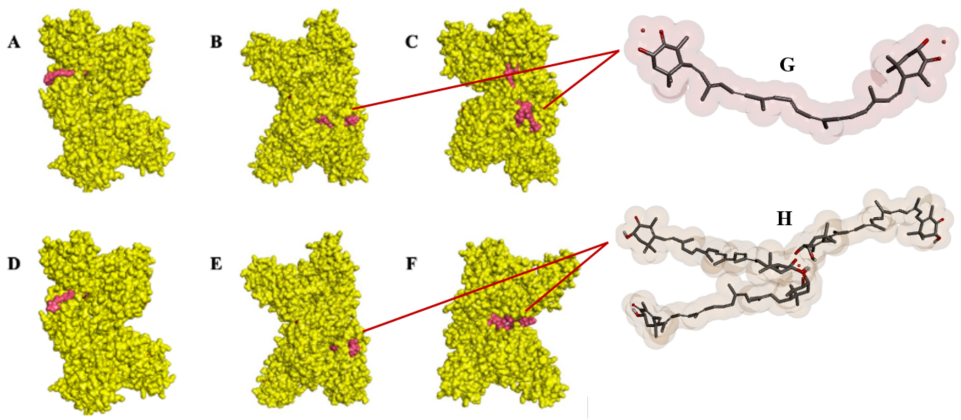

FIGURE 1 3D visualization of molecular docking results. (A) HSA and ASX; (B) HSA and ASX-Cu^{2+} (1:2); (C) HSA and ASX-Cu^{2+} (3:1); (D) gHSA and ASX; (E) gHSA and ASX-Cu^{2+} (1:2); (F) gHSA and ASX-Cu^{2+} (3:1); (G) molecular structure of the ASX-Cu^{2+} complex (1:2); (H) molecular structure of the ASX-Cu^{2+} complex (3:1).

TABLE 1 Comparative binding site analysis of molecular docking.

Amino Acid Residue	HSA + ASX	HSA + ASX-Cu^{2+} (1:2)	HSA + ASX-Cu^{2+} (3:1)	gHSA + ASX	gHSA + ASX-Cu^{2+} (1:2)	gHSA + ASX-Cu^{2+} (3:1)
LEU115	Alkyl	Alkyl	-	Alkyl	H-bond	Alkyl
ALA126	Alkyl	-	Alkyl	Alkyl	-	-
ILE142	Alkyl	Alkyl	-	Alkyl	Alkyl	-
PHE134	π-Alkyl	-	-	Alkyl	-	π-Alkyl
TYR138	π-Alkyl	π-Alkyl	-	π-Alkyl	-	-
LYS159	-	-	Alkyl	-	-	-
LYS162	-	-	Alkyl	-	-	-
VAL116	-	-	Alkyl	-	-	-
ARG117	-	-	Alkyl	-	-	Alkyl
PRO118	-	-	Alkyl	Alkyl	-	Alkyl
GLY189	-	-	-	H-bond	-	-
VAL122	-	-	-	Alkyl	-	-
MET123	-	-	-	Alkyl	-	-
ARG114	-	H-bond	-	-	H-bond	Alkyl
HIS146	-	-	H-bond	-	-	-
GLU565	-	-	H-bond	-	-	-
TYR140	-	-	-	-	Metal-acceptor	-
GLU141	-	-	-	-	Metal-acceptor	-

Interaction types: Alkyl, π-Alkyl, Conventional hydrogen bond (H-bond), Metal-acceptor. Absence of interaction is indicated by (-).

GLU141, TYR161, and ALA511. These results highlight that copper complexation not only enhances the binding strength of ASX to both native and glycated HSA but also introduces additional interaction sites, particularly through metal-acceptor bonding. This suggests that ASX-Cu^{2+} complexes may have enhanced potential for stabilizing HSA structure under glycation-induced stress, providing promising insights for therapeutic applications in oxidative stress and diabetes-related protein modification.

3.2. Molecular dynamic

The molecular dynamics simulations provided insights into the structural stability and flexibility of HSA and glycated HSA (gHSA) in both unbound and ligand-bound states. Native HSA maintained a relatively stable conformation throughout the simulation, reflecting its intrinsic structural robustness under physiological conditions. In contrast, gHSA showed increased fluctuations, indicating that glycation alters protein dynamics and reduces conformational stability, consistent with previous reports describing glycation-induced structural perturbations (Jeevanandam et al. 2024).

Upon binding with astaxanthin (ASX), both HSA and gHSA exhibited changes in molecular flexibility. In native HSA, ASX slightly reduced residue fluctuations, suggesting a moderate stabilizing effect mediated by hydrophobic interactions and hydrogen bonding (Yin et al. 2023). However, this stabilizing effect was less evident in gHSA, likely due to glycation-induced modifications that alter the binding environment and limit the formation of stabilizing interactions.

A more pronounced stabilization was observed upon formation of ASX-Cu^{2+} complexes (Shen et al. 2020). The HSA-ASX-Cu^{2+} (1:2) complex showed reduced RMSF values compared with both apo-HSA and HSA-ASX, indicating increased structural rigidity and compactness. This effect became more evident in the HSA-ASX-Cu^{2+} (3:1) complex, where the presence of multiple Cu^{2+} ions likely enhanced coordination with polar residues, forming a denser interaction network and further reducing backbone flexibility (Klaic et al. 2020).

Similarly, glycated HSA (gHSA) exhibited improved structural stability upon binding with ASX-Cu^{2+} complexes (Figure 2c and 2d). The gHSA-ASX-Cu^{2+} (1:2) complex showed lower RMSF values compared with gHSA and gHSA-ASX, indicating partial restoration of structural rigidity. A more pronounced stabilization was observed in the gHSA-ASX-Cu^{2+} (3:1) complex, where molecular fluctuations were reduced to levels comparable with native HSA. These results suggest that metal complexation enhances the interaction between ASX-Cu^{2+} and glycated residues, leading to a more ordered and stable protein conformation (Shen et al. 2020).

Overall, the molecular dynamics results indicate that copper coordination enhances the stabilizing capability of ASX toward both HSA and gHSA. The stabilization effect increased with the metal-to-ligand ratio, with the 3:1 complex producing the strongest reduction in structural fluctuations. This observation highlights the potential of ASX-Cu^{2+} complexes to restore or maintain the structural integrity of proteins affected by glycation.

The RMSF data illustrate how the interaction between ASX-Cu^{2+} and both HSA and gHSA affects protein flexibility at the residue level, providing a deeper understand-

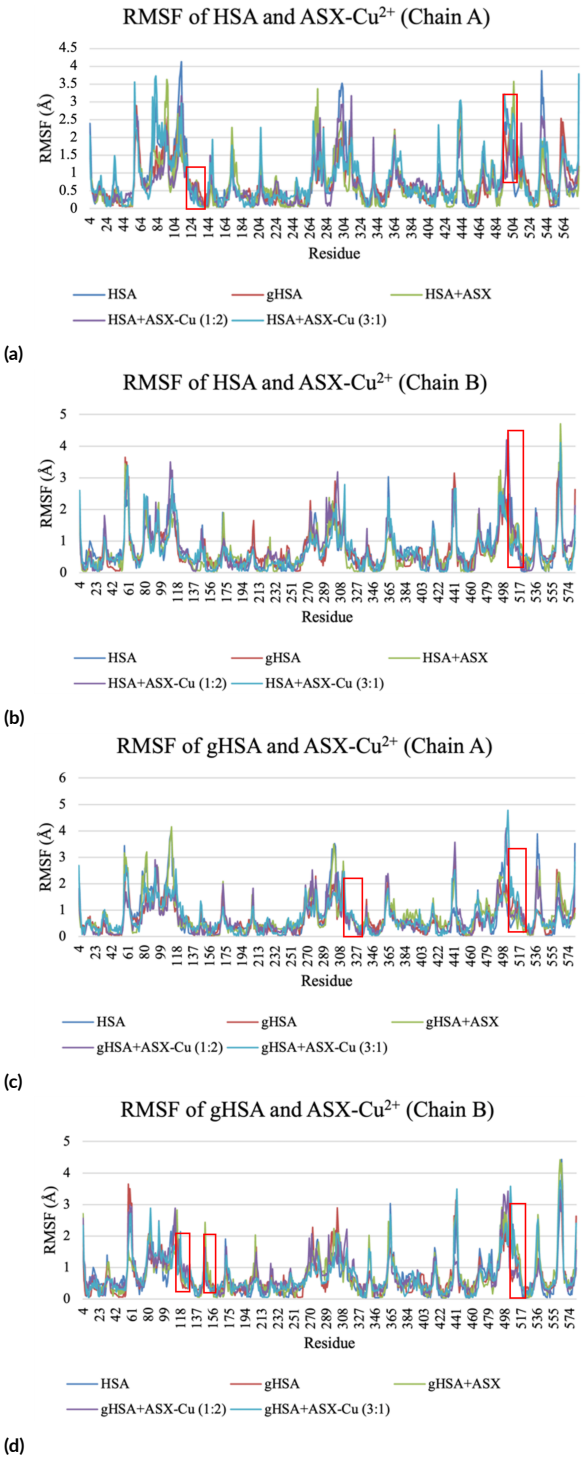

FIGURE 2 Root mean square fluctuation (RMSF) graph result. (a) RMSF of HSA and ASX-Cu^{2+} (Chain A); (b) RMSF of HSA and ASX-Cu^{2+} (Chain B); (c) RMSF of gHSA and ASX-Cu^{2+} (Chain A); (d) RMSF of gHSA and ASX-Cu^{2+} (Chain B). Red boxes indicate residue regions exhibiting significant changes in RMSF upon ligand binding, highlighting segments that undergo notable stabilization or altered flexibility in the ASX-Cu^{2+} complexes.

ing of the stabilizing role of the metal complex. In general, lower RMSF values indicate greater structural rigidity and stability, while higher values suggest increased flexibility or local unfolding. The red boxes highlighted in the RMSF profiles indicate specific residue regions that exhibit pronounced changes in flexibility upon ligand binding. These regions correspond to segments showing a marked reduction in RMSF values in the ASX-Cu^{2+} complexes compared to unbound or ASX-bound HSA/gHSA systems, suggesting local structural stabilization induced by ligand interaction. Such reductions in residue-level fluctuations are commonly associated with the involvement of these regions in ligand binding interfaces or with allosteric effects propagating from the binding site.

In the HSA-ASX-Cu^{2+} complex, both Chain A and Chain B showed reduced fluctuations compared with unbound or ASX-bound HSA (Figure 2a and 2b). In Chain A, RMSF suppression was observed in ligand-binding regions, particularly around key residues Leu115, Ile142, and Tyr138 (Figure 2a). Additional decreases in RMSF were detected at residues 495 and 497, suggesting their involvement in the binding interface or allosteric stabilization induced by the ASX-Cu^{2+} complex. These reductions indicate that metal-assisted ligand binding promotes structural rigidity in regions important for ligand and metal coordination.

Chain B exhibited a moderate but consistent stabilization effect (Figure 2b), although less pronounced than in Chain A. Significant RMSF reductions were observed in residues Arg10, Phe11, Lys12, and Asp13, which are known to participate in transition metal coordination. Additional stabilization was detected near the C-terminal domain, particularly at residues Phe508, His509, and Ser578, suggesting either direct interaction with the ligand or allosteric stabilization within the binding region. Together, these results indicate that ASX-Cu^{2+} complexation contributes to the stabilization of key structural regions in HSA.

The effect of gHSA + ASX-Cu^{2+} complex was also noticeable with different dynamics. Chain A of gHSA displayed an appreciable reduction in RMSF values compared to native gHSA (Figure 2c), particularly in regions previously destabilized by glycation. This finding indicates that ASX-Cu^{2+} not only binds effectively to gHSA but also mitigates glycation-induced flexibility by reinforcing structural stability through metal coordination and aromatic interactions. Chain B of gHSA, however exhibited a more modest reduction in RMSF values (Figure 2d), suggesting partial stabilization.

In the Chain A gHSA-ASX-Cu^{2+} complex, significant RMSF suppression was observed in several regions (Figure 2c). A notable reduction occurred within residues 110-125, including His117, a known metal-coordinating residue in albumin, suggesting direct involvement in Cu^{2+} coordination or stabilization of the ASX-Cu^{2+} complex. Additional decreases in flexibility were detected in regions 210-230 (Ala213, Lys225, Glu227), 310-330 (Lys313, Arg318, Gln323), and 470–490 (Glu476, Asp478, Lys490), the latter corresponding to domain III of albumin associated with metal binding and structural transitions. These results indicate that ASX-Cu^{2+} binding stabilizes both the primary binding pocket

and distal structural regions, suggesting long-range conformational stabilization.

In Chain B of the gHSA-ASX-Cu^{2+} complex (Figure 2d), several residues also showed pronounced reductions in flexibility compared with the apo and ASX-bound forms. Suppression was observed near the high-affinity metal-binding site around Gln33 and Cys34, indicating their potential involvement in Cu^{2+} coordination. Additional stabilization occurred in the Arg114-Val116 region, where Arg114 exhibited the largest RMSF reduction, suggesting participation in ionic or hydrogen-bond interactions with ASX or Cu^{2+}. Reduced mobility was also detected in the Pro147-Tyr153 region, including Tyr148 and Tyr150, which may participate in π-π stacking interactions with the conjugated system of ASX. Furthermore, the aromatic residue Phe206 showed strong RMSF suppression, indicating potential hydrophobic or stacking interactions that contribute to ligand stabilization and orientation.

3.3. Gyration analysis

The asphericity, radius of gyration (Rg), and total hydration analyses collectively describe the structural compactness and solvent exposure of the protein during the simulation (Figure 3a-c). Lower asphericity and Rg values indicate a more compact and spherical conformation, while reduced hydration reflects decreased solvent-accessible surface area. In the HSA-ASX-Cu^{2+} complex, all three parameters remained consistently low and stable throughout the simulation, indicating that the protein maintained a compact and structurally stable conformation. This behavior suggests that Cu^{2+} coordination with ASX reinforces intramolecular interactions, limits anisotropic deformation, and restricts surface flexibility, thereby preserving the native tertiary structure of HSA (Hollingsworth and Dror 2018; De Vivo et al. 2016). In contrast, the gHSA-ASX-Cu^{2+} complex initially exhibited higher asphericity, Rg, and hydration values, reflecting glycation-induced structural loosening and increased solvent exposure. However, all three parameters gradually decreased during the simulation, indicating that ASX-Cu^{2+} binding promotes a shift toward a more ordered and compact conformation. Although the final structural compactness did not fully reach that of native HSA, these results suggest that the ASX-Cu^{2+} complex partially restores the structural stability of glycated HSA by reducing conformational expansion and solvent accessibility. Overall, the combined analysis indicates that ASX-Cu^{2+} contributes to stabilizing both native and glycated albumin, with a stronger stabilizing effect observed in native HSA.

The fractional ratio (f/f_0), excluded volume (Bex), and axial ratio collectively describe the hydrodynamic compactness and geometric shape of protein-ligand complexes during the simulation (Figure 3d–f). Lower f/f_0 values and axial ratios approaching unity indicate a more compact and spherical conformation, while stable Bex values reflect preservation of the protein's three-dimensional structural volume. In the HSA-ASX-Cu^{2+} complex, these parameters remained relatively low and stable throughout the simulation, indicating that the protein maintained a compact globular structure and consistent spatial organization. This behavior suggests that coordination between ASX and Cu^{2+} restricts structural fluctuations and reinforces intramolecular interactions, thereby preserving the native hydrodynamic properties of HSA. In contrast, the gHSA-ASX-Cu^{2+} complex initially exhibited higher f/f_0 and axial ratio values together with greater Bex variability, reflecting glycation-induced structural distortion and increased conformational flexibility. However, these parameters gradually decreased during the simulation, indicating that ASX-Cu^{2+} binding promotes a progressive shift toward a more compact and ordered conformation. Although the final values remained slightly higher than those observed for native HSA, the results suggest that the ASX-Cu^{2+} complex partially restores the hydrodynamic compactness and structural stability of glycated HSA.

The diffusion coefficient (Dt), sedimentation coefficient (s_{20},w), and rotational correlation time (τc) collectively describe the hydrodynamic mobility and rotational behavior of protein-ligand complexes in solution (Figure 3g–i). Higher Dt and s_{20},w values together with lower τc generally indicate a more compact and hydrodynamically efficient structure, whereas the opposite trends reflect structural expansion and reduced compactness. In the HSA-ASX-Cu^{2+} complex, Dt and s_{20},w remained relatively high while τc stayed low and stable throughout the simulation, indicating that the protein maintained a compact and structurally stable conformation. These trends suggest that coordination between ASX and Cu^{2+} reinforces intramolecular interactions and preserves the globular architecture of HSA, consistent with the compact structural behavior observed in previous gyration and shape analyses. In contrast, the gHSA-ASX-Cu^{2+} complex initially exhibited lower Dt and s_{20},w values together with higher τc, reflecting glycation-induced structural expansion and reduced hydrodynamic efficiency. However, during the simulation Dt and s_{20},w gradually increased while τc decreased, indicating a progressive shift toward a more compact conformation upon ASX-Cu^{2+} binding. Although the final values did not fully match those of native HSA, these results suggest that the ASX-Cu^{2+} complex partially restores the hydrodynamic compactness and dynamic stability of glycated HSA.

3.4. The free energy landscape (FEL)

The free energy landscape (FEL) projected onto the first two principal components (PC1 and PC2) provides insight into the conformational stability and flexibility of human serum albumin during the simulation (Figure 4a). Native HSA exhibits a well-defined global minimum around PC1 (–15 to 5) and PC2 (–10 to 5) with a minimum free energy of approximately –8.3 kJ/mol, indicating a dominant thermodynamically stable conformation with a smooth surrounding energy gradient that reflects gradual transitions between states. This pattern suggests that HSA maintains structural stability while retaining moderate conformational flexibility. In contrast, upon binding with astax-

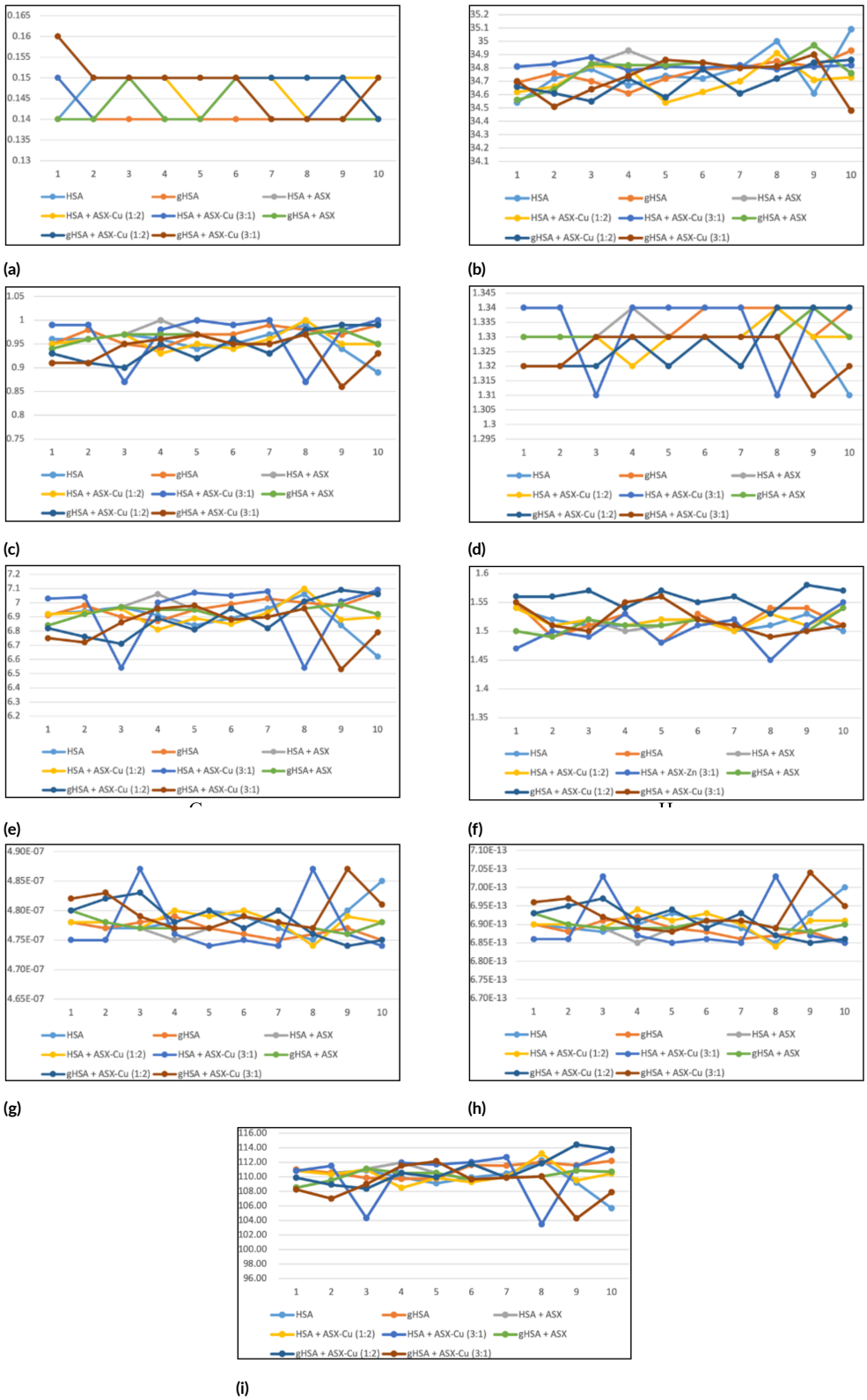

FIGURE 3 Gyration analysis. (a) Asphericity; (b) Radius of gyration (RG); (c) Total hydration; (d) f/fo (Fractional ratio); (e) Bex (excluded volume); (f) Axial ratio; (g) Dt (Diffusion coefficient); (h) s20 (Sedimentation coefficient); (i) tauC (Rotational correlation time).

anthin (ASX), the FEL becomes broader and more evenly distributed across the PC space (–30 to 30) with free energy values ranging from about –8.0 to –10.7 kJ/mol. The global minimum becomes less pronounced and multiple shallow basins emerge, indicating increased conformational sampling and the presence of several metastable states. This behavior suggests that ASX binding enhances structural flexibility and allows HSA to access a wider

range of conformational states that may facilitate ligand accommodation.

The FEL analysis of HSA complexes reveals distinct stability patterns depending on the ASX-Cu^{2+} coordination ratio (Figure 4a). The HSA-ASX-Cu^{2+} complex at a 1:2 ratio exhibits a well-defined global minimum located near PC1 (0–10) and PC2 (–10–0), indicating stabilization of a dominant low-energy conformation. Although the conformational space remains moderately broad, the energy basin becomes deeper and more localized compared with the HSA-ASX complex, suggesting that Cu^{2+} coordination enhances structural stability while maintaining necessary flexibility. The presence of several shallow local minima further indicates metastable states that may represent intermediate conformations during ligand-metal-protein interactions. In contrast, the HSA-ASX-Cu^{2+} complex at a 3:1 ratio displays a shallower and more dispersed energy basin with free energy values between approximately –7.9 and –10.5 kJ/mol, reflecting a more heterogeneous conformational ensemble and reduced structural specificity. This broader distribution likely arises from excess Cu^{2+} perturbing the optimal coordination environment. Overall, these results indicate that the ASX-Cu^{2+} complex at a 1:2 ratio provides the most favorable balance between structural stability and conformational flexibility in HSA.

The more focused FEL topology with a deep and localized global minimum observed at the 1:2 ratio aligns well with the concept that well-defined Cu^{2+} coordination stabilizes a dominant low-energy state while still allowing a few shallow metastable states to exist as intermediates (Charette et al. 2022). Molecular dynamics studies of the copper-binding protein Atox1 have shown that a "complete" coordination state (four-coordinate geometry) results in a more rigid and organized conformation, whereas reduced or suboptimal coordination increases flexibility and enriches metastable states within the PC1/PC2 conformational space (Schwartz et al. 2022). In HSA/ASX/metal ion systems, combined EPR, CD, and MD analyses indicate that the formation of Cu^{2+} complexes with well-defined coordination geometry produces structures that are both stable and dynamically adaptable, with several

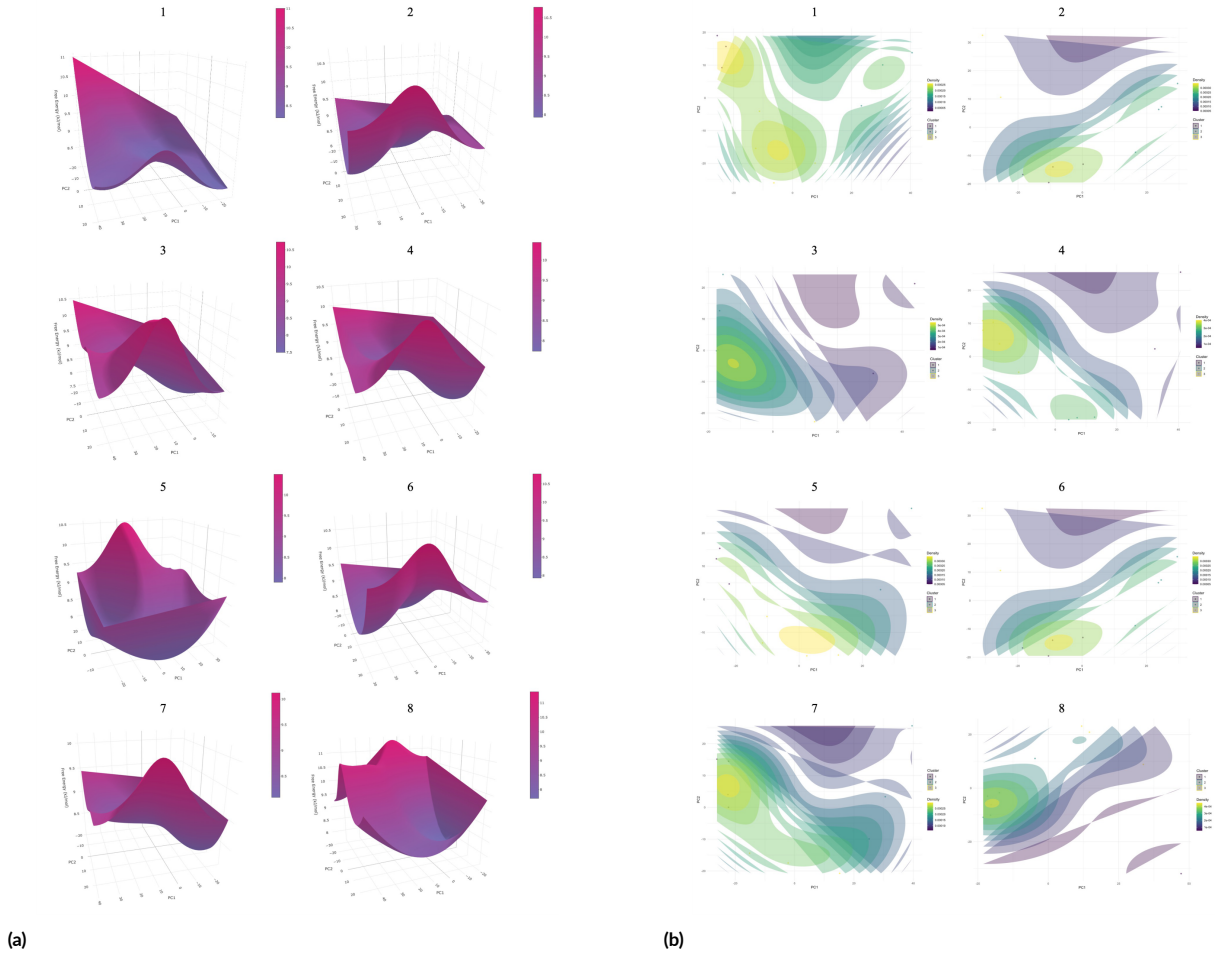

FIGURE 4 (a) Free energy landscape (FEL) represented as 3D surface plots, showing the energy basins and conformational stability of each complex: (1) HSA; (2) HSA + ASX; (3) HSA + ASX-Cu^{2+} (1:2); (4) HSA + ASX-Cu^{2+} (3:1); (5) gHSA; (6) gHSA + ASX; (7) gHSA + ASX-Cu^{2+} (1:2); (8) gHSA + ASX-Cu^{2+} (3:1). (b) 2D free energy landscape (FEL) with cluster overlay from molecular dynamics simulation projections (PC1 vs PC2), highlighting the conformational clusters and energy minima: (1) HSA; (2) HSA + ASX; (3) HSA + ASX-Cu^{2+} (1:2); (4) HSA + ASX-Cu^{2+} (3:1); (5) gHSA; (6) gHSA + ASX; (7) gHSA + ASX-Cu^{2+} (1:2); (8) gHSA + ASX-Cu^{2+} (3:1).

metastable conformations relevant to metal transfer processes and ligand-protein interactions (Koshenskova et al. 2025). This interpretation is consistent with the presence of several shallow local minima surrounding the main basin in the 3D FEL.

In contrast, at the 3:1 ratio, several studies suggest that excess Cu^{2+} or "over-saturated" coordination geometries tend to increase conformational heterogeneity and the dynamic behavior of the complex. In Atox1, alterations or reductions in Cu(I) coordination patterns have been shown to increase global flexibility and broaden the distribution of conformational states across the PC1/PC2 space (Schwartz et al. 2022). Other Cu(II) complexes with organic ligands similarly demonstrate that variations in the number and type of coordinating ligands promote conformer interconversion and lead to shallower energy minima, which are reflected in more flexible spectral and redox behaviors (Griffin et al. 2023).

The 2D free energy landscape (FEL) of glycated human serum albumin (gHSA) projected onto PC1 and PC2 reveals a relatively narrow conformational distribution with a pronounced global minimum (Figure 4b). The free energy ranges from approximately –7.9 to –10.5 kJ/mol, forming a deep basin that indicates a dominant and relatively rigid conformational state. This pattern suggests that glycation restricts structural flexibility and limits the accessible conformational space of HSA. Upon binding with astaxanthin (ASX), the FEL becomes broader and smoother, indicating increased conformational sampling. The energy minima are distributed across a wider PC space (–30 to 30), suggesting that ASX partially restores structural plasticity in gHSA by allowing the protein to access multiple metastable conformations.

The gHSA-ASX-Cu^{2+} complex at a 1:2 ratio displays a moderately rugged landscape with a distinct global minimum (–8.4 to –10.2 kJ/mol). Compared with gHSA alone, this system shows greater conformational diversity but remains relatively organized, indicating that copper coordination together with ASX promotes structural stabilization while maintaining necessary flexibility. In contrast, the gHSA-ASX-Cu^{2+} complex at a 3:1 ratio exhibits a more rugged FEL with multiple local minima and broader conformational sampling (PC1 ≈ –20 to 45; PC2 ≈ –30 to 20). The wider energy distribution suggests increased conformational heterogeneity and possible destabilization caused by excess Cu^{2+} ions, which may perturb optimal ligand coordination.

The finding that the gHSA-ASX-Cu^{2+} complex at a 1:2 ratio maintains a well-defined global minimum while exhibiting moderate conformational diversity is consistent with EPR spectroscopic observations and dynamical studies showing that Cu^{2+} coordination by albumin and organic ligands can stabilize protein structure while preserving functional flexibility (Chen et al. 2019). In contrast, the interpretation that the 3:1 ratio produces a more rugged free energy landscape (FEL) with multiple local minima and greater conformational heterogeneity is supported by studies demonstrating that increased metal ion concentrations can alter coordination geometry, introduce alternative binding pathways, and enrich transition routes across the free energy landscape (Wang et al. 2022).

The comparison with native HSA indicates that the gHSA-ASX-Cu^{2+} (1:2) complex most closely resembles the native conformational landscape, maintaining a balanced combination of stability and flexibility. The cluster overlay further highlights several dominant conformational states within the FEL, representing stable and intermediate conformers sampled during the simulation. These results suggest that the 1:2 ASX-Cu^{2+} complex provides the most favorable structural stabilization of glycated HSA.

The approximate fuzzy entropy based on Shannon entropy values describes the conformational variability of HSA and gHSA systems under different ligand and Cu^{2+} conditions (Figure 5). Native HSA shows the lowest entropy (1.8673), indicating a stable and less flexible structure. Glycation increases the entropy to 2.3494, suggesting higher structural disorder in gHSA. The addition of

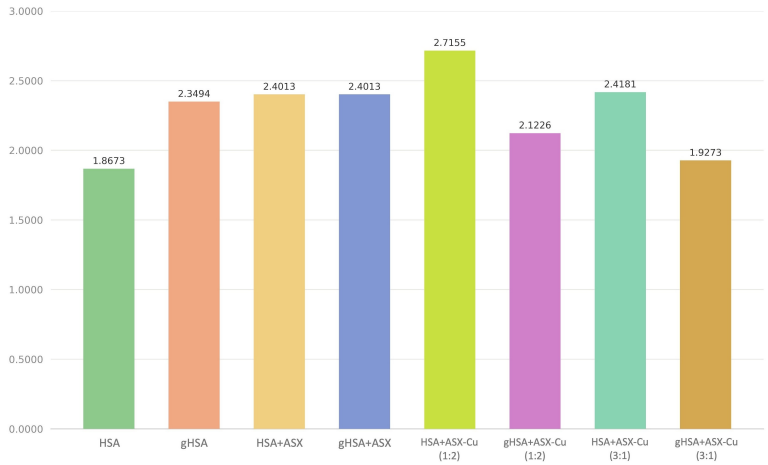

FIGURE 5 Shannon entropy (nat) derived from approximate fuzzy entropy analysis for HSA, gHSA, and their complexes with astaxanthin (ASX) and ASX-Cu^{2+} (1:2 and 3:1).

ASX slightly increases entropy in both HSA and gHSA systems (2.4013), indicating modest increases in conformational flexibility upon ligand binding.

The HSA-ASX-Cu^{2+} complex at a 1:2 ratio exhibits the highest entropy (2.7155), suggesting greater conformational heterogeneity likely induced by combined ligand-metal interactions. In contrast, the corresponding gHSA complex shows lower entropy (2.1226), indicating that glycation may limit structural fluctuations. At the 3:1 ASX:Cu^{2+} ratio, entropy values decrease for both HSA and gHSA systems (2.4181 and 1.9273), suggesting that excess ASX may partially stabilize the protein structure. Overall, the results indicate that glycation, ligand binding, and Cu^{2+} coordination collectively modulate the conformational entropy and structural dynamics of albumin.

3.5. The residue interaction network (RIN)

The residue interaction network (RIN) of HSA illustrates the non-covalent interactions that maintain the structural organization of the protein (Figure 6a). In this network,

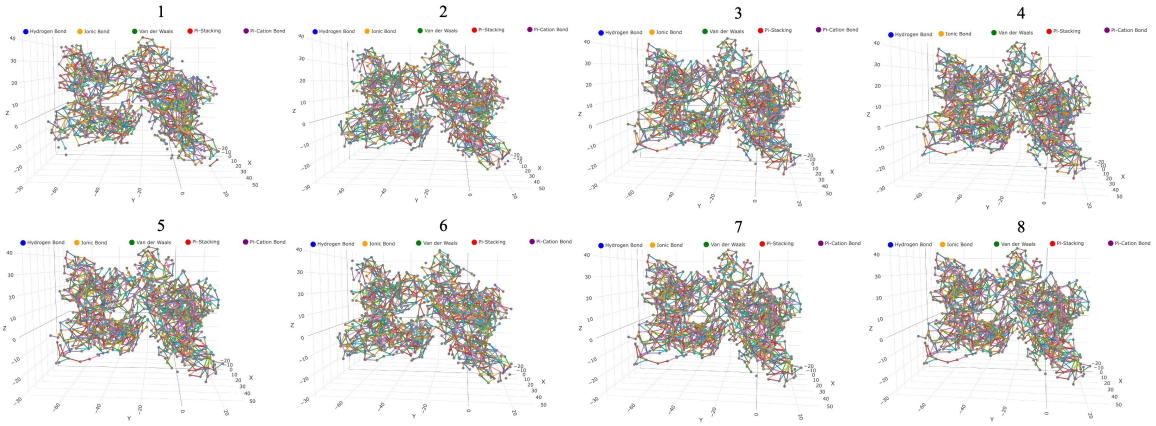

(a)

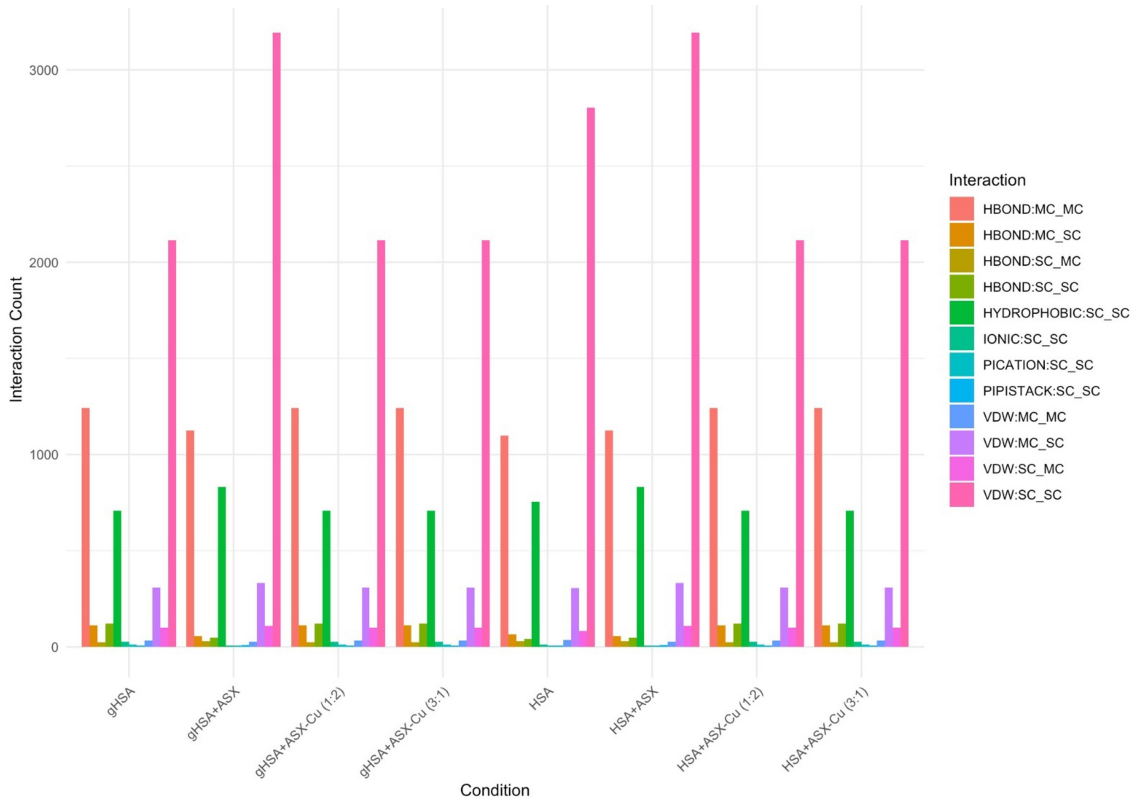

(b)

FIGURE 6 (a) Residue interaction network (RIN) showing the 3D topology of intra-protein interactions in each system, with interaction types color-coded on the protein structure: (1) HSA; (2) HSA + ASX; (3) HSA + ASX-Cu^{2+} (1:2); (4) HSA + ASX-Cu^{2+} (3:1); (5) gHSA; (6) gHSA + ASX; (7) gHSA + ASX-Cu^{2+} (1:2); (8) gHSA + ASX-Cu^{2+} (3:1). (b) Comparison of interaction types across the systems, showing the number of hydrogen bonds, hydrophobic contacts, van der Waals interactions, ionic bonds, and aromatic interactions (π-π and cation-π), classified by main-chain (MC) and side-chain (SC) residues.

nodes represent amino acid residues and edges indicate interaction types, including hydrogen bonds (blue), ionic interactions (orange), van der Waals contacts (green), π-stacking (red), and π-cation interactions (purple). The dense connectivity of the network reflects strong intramolecular communication that stabilizes the protein structure. Hydrogen bonds and van der Waals interactions are the most dominant, indicating their primary role in maintaining the compact fold of HSA, while aromatic interactions such as π-stacking and π-cation contacts provide additional stabilization and may contribute to ligand recognition.

In the HSA-astaxanthin (ASX) complex, the RIN shows increased interaction density compared with native HSA (Figure 6b). In particular, π-stacking and π-cation interactions become more prominent, suggesting that ASX binding enhances aromatic and electrostatic contacts with nearby residues. This behavior is consistent with the conjugated polyene structure of ASX, which facilitates multiple non-covalent interactions and may induce local conformational adjustments within ligand-binding regions.

For the HSA-ASX-Cu^{2+} (1:2) complex, the RIN reveals a further reorganization of the interaction network. Ionic and π-cation interactions become more pronounced, likely due to coordination between Cu^{2+} ions and electron-rich residues near the binding pocket. This results in a denser interaction network, supported by additional van der Waals and π-stacking contacts involving aromatic residues. Overall, the combined presence of ASX and Cu^{2+} strengthens the internal interaction network of HSA, suggesting enhanced structural stabilization and modified ligand-interaction properties.

The interaction profile of HSA and glycated HSA (gHSA) under different ligand (ASX) and Cu^{2+} conditions revealed distinct molecular interaction patterns. Across all systems, van der Waals interactions between side chains (VDW:SC_SC) were the most dominant, indicating that dispersion forces play a major role in stabilizing protein structure and mediating ligand binding. Hydrogen bonds, particularly HBOND:MC_MC and HBOND:SC_MC, were also consistently observed and contributed to maintaining local structural stability. However, gHSA complexes exhibited a slight reduction in HBOND:MC_SC interactions compared with native HSA, suggesting that glycation alters the hydrogen-bonding network and protein flexibility. Previous studies have shown that glycation modifies HSA domain dynamics, the geometry of the ligand-binding pocket (Sudlow site I), and the internal hydrogen-bonding network, leading to increased global flexibility, reduced α-helix content in the ligand-binding region, and changes in pocket volume and hydration (Sittiwanichai et al. 2023). These structural changes can also shift the positioning of key residues such as W214, K195, and Cys34 and reorganize inter-residue interaction patterns around the binding site, explaining the reduced hydrogen-bond fraction and redistribution of van der Waals and polar interactions observed in the gHSA residue interaction network (Tadawattana et al. 2025).

Consistent with these observations, glycation has been reported to reduce the affinity of HSA for metal ions such as Cu^{2+} and Zn^{2+} through modification of the N-terminal metal-binding motif (NTS/DAHK), although cooperativity among metal-binding sites generally remains preserved (Pomier et al. 2024). These changes in domain dynamics, ligand-pocket geometry, and metal coordination provide a structural basis for the looser and less coordinated RIN pattern observed in gHSA compared with native HSA, supporting the reduced HBOND:MC_SC contribution and increased flexibility in the glycated system (Escobosa et al. 2015). In the HSA-ASX-Cu^{2+} complexes, the 1:2 ratio exhibited a balanced interaction network between hydrogen bonds and van der Waals contacts, indicating stable yet flexible ligand binding. In contrast, the 3:1 ratio showed increased VDW:SC_SC interactions with relatively fewer hydrogen bonds, suggesting tighter side-chain packing and a more hydrophobic interaction environment that may enhance structural rigidity while reducing flexibility. A similar trend was observed in gHSA complexes, where the 1:2 ASX-Cu^{2+} ratio maintained a balanced interaction profile, whereas the 3:1 ratio further increased van der Waals interactions, reflecting stronger side-chain packing and structural compaction, consistent with hydrophobic stabilization mechanisms in proteins (Dill and MacCallum 2012).

Overall, van der Waals interactions remain the primary stabilizing force in all systems, while glycation modifies the hydrogen-bonding network and interaction balance. The 1:2 ASX-Cu^{2+} ratio provides a more balanced interaction profile that maintains structural stability without excessive rigidity, whereas the 3:1 ratio promotes stronger hydrophobic packing and reduced interaction flexibility (Keserü and Makara 2009; Chandler 2005).

4. Conclusions

The ASX-Cu^{2+} (1:2) complex demonstrates a robust capacity to stabilize both native and glycated human serum albumin, addressing the structural disruptions caused by glycation. Compared to free astaxanthin and other ASX-Cu^{2+} ratios, the 1:2 complex consistently improves binding affinity, reduces conformational flexibility, and promotes a more compact, globular protein structure. These findings are reinforced by molecular docking, dynamics simulations, FEL mapping, and residue interaction analyses, all pointing to enhanced structural integrity and functional resilience. The ability of ASX-Cu^{2+} (1:2) to restore near-native conformations in glycated HSA highlights its potential as a targeted bioinorganic strategy for mitigating protein dysfunction in oxidative and diabetic conditions.

Acknowledgments

We would like to express our sincere gratitude to the RIIM Invitasi Strategis Platform Biologi Struktur for providing the research funding.

Authors' contributions

NA, AF wrote the manuscript. SW, JES, BWKW, CSB, TRN carried out virtual screening and analyzed the data. IMA, SW supervised and designed the experiment and the manuscript.

Competing interests

There were no conflicts of interest in this article.

References

Ambati RR, Moi PS, Ravi S, Aswathanarayana RG. 2014. Astaxanthin: sources, extraction, stability, biological activities and its commercial applications—a review. Mar. Drugs 12(1):128–152. doi:10.3390/md12010128.

Chandler D. 2005. Interfaces and the driving force of hydrophobic assembly. Nature 437(7059):640–647. doi:10.1038/nature04162.

Charette BJ, Griffin PJ, Zimmerman CM, Olshansky L. 2022. Conformationally dynamic copper coordination complexes. Dalton Trans. 51(16):6212–6219. doi:10.1039/D2DT00312K.

Chen K, Li W, Wang J, Wang W. 2019. Binding of copper ions with octapeptide region in prion protein: simulations with charge transfer model. J. Phys. Chem. B 123(25):5216–5228. doi:10.1021/acs.jpcb.9b02457.

De Simone G, di Masi A, Ascenzi P. 2021. Serum albumin: a multifaced enzyme. Int. J. Mol. Sci. 22(18):10086. doi:10.3390/ijms221810086.

De Vivo M, Masetti M, Bottegoni G, Cavalli A. 2016. Role of molecular dynamics and related methods in drug discovery. J. Med. Chem. 59(9):4035–4061. doi:10.1021/acs.jmedchem.5b01684.

Dill KA, MacCallum JL. 2012. The protein-folding problem, 50 years on. Science 338(6110):1042–1046. doi:10.1126/science.1219021.

Escobosa AR, Wrobel K, Yanez Barrientos E, Jaramillo Ortiz S, Ramirez Segovia AS, Wrobel K. 2015. Effect of different glycation agents on Cu (II) binding to human serum albumin, studied by liquid chromatography, nitrogen microwave-plasma atomic-emission spectrometry, inductively-coupled-plasma mass spectrometry, and high-resolution molecular-mass spectrometry. Anal. Bioanal. Chem. 407(4):1149–1157. doi:10.1007/s00216-014-8335-1.

Fleming PJ, Fleming KG. 2018. HullRad: fast calculations of folded and disordered protein and nucleic acid hydrodynamic properties. Biophys. J. 114(4):856–869. doi:10.1016/j.bpj.2018.01.002.

Griffin PJ, Dake MJ, Remolina AD, Olshansky L. 2023. Conformational dynamicity in a copper (II) coordination complex. Dalton Trans. 52(24):8376–8383. doi:10.1039/D3DT01213A.

Guérin M, Huntley ME, Olaizola M. 2003. *Haematococcus astaxanthin*: applications for human health and nutrition. Trends Biotechnol. 21(5):210–216. doi:10.1016/S0167-7799(03)00078-7.

Hollingsworth SA, Dror RO. 2018. Molecular dynamics simulation for all. Neuron 99(6):1129–1143. doi:10.1016/j.neuron.2018.08.011.

Jamroz M, Kolinski A, Kmiecik S. 2013. CABS-flex: server for fast simulation of protein structure fluctuations. Nucleic Acids Res. 41(W1):W427–W431. doi:10.1093/nar/gkt332.

Jeevanandam J, Barhoum A, Danquah MK, Nordin NAHM. 2024. Glycation of human serum albumin: implications for drug binding and protein function. Biochem. Pharmacol. 213:115552. doi:10.1016/j.bcp.2023.115552.

Ke G, Hu P, Xiong H, Zhang J, Xu H, Xiao C, Zheng Q. 2025. Enhancing temozolomide efficacy in GBM: the synergistic role of chuanxiong rhizoma essential oil. Phytomedicine 140:156575. doi:10.1016/j.phymed.2025.156575.

Keserü GM, Makara GM. 2009. The influence of lead discovery strategies on the properties of drug candidates. Nat. Rev. Drug Discov. 8(3):203–212. doi:10.1038/nrd2796.

Khalid M, Petroianu G, Adem A. 2022. Advanced glycation end products and diabetes mellitus: mechanisms and perspectives. Biomolecules 12(4):542. doi:10.3390/biom12040542.

Klaic L, Vukelic I, Planinic P. 2020. Structural and antioxidant evaluation of natural products coordinated with transition metals: a DFT study. J. Inorg. Biochem. 209:111105.

Koshenskova KA, Makarenko NV, Dolgushin FM, Yambulatov DS, Bekker OB, Fedin MV, Lutsenko IA. 2025. Green-ligand in metallodrugs design—Cu (II) complex with phytic acid: synthetic approach, EPR-spectroscopy, and antimycobacterial activity. Molecules 30(2):313. doi:10.3390/molecules30020313.

Kuriata A, Gierut AM, Oleniecki T, Ciemny MP, Kolinski A, Kurcinski M, Kmiecik S. 2018. CABS-flex 2.0: a web server for fast simulations of flexibility of protein structures. Nucleic Acids Res. 46(W1):W338–W343. doi:10.1093/nar/gky356.

Liu Y, Yang X, Gan J, Chen S, Xiao ZX, Cao Y. 2022. CB-Dock2: improved protein-ligand blind docking by integrating cavity detection, docking and homologous template fitting. Nucleic Acids Res. 50(W1):W159–W164. doi:10.1093/nar/gkac394.

Pomier KM, Ahmed R, Huang J, Melacini G. 2024. Inhibition of toxic metal-alpha synuclein interactions by human serum albumin. Chem. Sci. 15(10):3502–3515. doi:10.1039/D3SC06285F.

Schwartz R, Ruthstein S, Major DT. 2022. Copper coordination states affect the flexibility of copper metallochaperone Atox1: insights from molecular dynamics simulations. Protein Sci. 31(12):e4464.

doi:10.1002/pro.4464.

Shen L, Yang W, Wang D, Yu Y, Chen L. 2020. Metal coordination of astaxanthin in BioMOFs: structure and antioxidant performance. J. Mol. Struct. 1203:127429. doi:10.1016/j.molstruc.2019.127429.

Sittel F, Stock G. 2018. Perspective: identification of collective variables and metastable states of protein dynamics. J. Chem. Phys. 149(15):150901. doi:10.1063/1.5049637.

Sittiwanichai S, Japrung D, Mori T, Pongprayoon P. 2023. Structural and dynamic alteration of glycated human serum albumin in schiff base and Amadori adducts: a molecular simulation study. J. Phys. Chem. B 127(23):5230–5240. doi:10.1021/acs.jpcb.3c02048.

Tadawattana P, Sittiwanichai S, Japrung D, Pongprayoon P. 2025. The effect of full glycation on structure and function of human serum albumin. J. Biomol. Struct. Dyn. p. 1–11. doi:10.1080/07391102.2025.2578688.

Tiberti M, Piovesan D, Remondini D, Fariselli P, Martelli PL. 2022. RINmaker: a web server to compute and visualize residue interaction networks from protein structures. Bioinformatics 38(4):1147–1149. doi:10.1093/bioinformatics/btab800.

Valko M, Leibfritz D, Moncol J, Cronin MT, Mazur M, Telser J. 2007. Free radicals and antioxidants in normal physiological functions and human disease. Int. J. Biochem. Cell Biol. 39(1):44–84. doi:10.1016/j.biocel.2006.07.001.

Wang J, Ishchenko A, Zhang W, Razavi A, Langley D. 2022. A highly accurate metadynamics-based dissociation free energy method to calculate protein-protein and protein-ligand binding potencies. Sci. Rep. 12(1):2024. doi:10.1038/s41598-022-05875-8.

Wibowo S, Costa J, Baratto MC, Pogni R, Widyarti S, Sabarudin A, Sumitro SB. 2022. Quantification and improvement of the dynamics of human serum albumin and glycated human serum albumin with astaxanthin/astaxanthin-metal ion complexes: physico-chemical and computational approaches. Int. J. Mol. Sci. 23(9):4771. doi:10.3390/ijms23094771.

Yin M, Liu H, Huang Y, Liu Y, Zhao J. 2023. Unraveling the underlying mechanism of interactions between astaxanthin geometrical isomers and bovine serum albumin. J. Mol. Liq. 380:122784. doi:10.1016/j.molliq.2023.122784.